



COMMUNICATIONS BIOLOGY

ARTICLE

<https://doi.org/10.1038/s42003-020-01279-4>

OPEN



High pressures increase α -chymotrypsin enzyme activity under perchlorate stress

Stewart Gault  ¹✉, Michel W. Jaworek  ², Roland Winter  ² & Charles S. Cockell  ¹

Deep subsurface environments can harbour high concentrations of dissolved ions, yet we know little about how this shapes the conditions for life. We know even less about how the combined effects of high pressure influence the way in which ions constrain the possibilities for life. One such ion is perchlorate, which is found in extreme environments on Earth and pervasively on Mars. We investigated the interactions of high pressure and high perchlorate concentrations on enzymatic activity. We demonstrate that high pressures increase α -chymotrypsin enzyme activity even in the presence of high perchlorate concentrations. Perchlorate salts were shown to shift the folded α -chymotrypsin phase space to lower temperatures and pressures. The results presented here may suggest that high pressures increase the habitability of environments under perchlorate stress. Therefore, deep subsurface environments that combine these stressors, potentially including the subsurface of Mars, may be more habitable than previously thought.

¹UK Centre for Astrobiology, SUPA School of Physics and Astronomy, University of Edinburgh, James Clerk Maxwell Building, Peter Guthrie Tait Road, Edinburgh EH9 3FD, UK. ²Faculty of Chemistry and Chemical Biology, Physical Chemistry I - Biophysical Chemistry, TU Dortmund University, Otto-Hahn-Str. 4a, D-44227 Dortmund, Germany. ✉email: s.a.gault@sms.ed.ac.uk

When searching for habitable environments elsewhere in the cosmos, one criterion is to seek liquid water. This is well grounded in our understanding of the importance of an appropriate solvent for the processes of life to occur in ref. ¹. Therefore on Mars, much attention has been paid to environments where evidence of liquid water has been observed or is predicted to exist^{2,3}. However, the mere presence of liquid water does not make an environment habitable. How life responds to external physical and chemical factors such as temperature, pressure, pH, and salinity will also define the edges of habitability^{4,5}.

On Mars, prime candidates for habitable environments are deep aqueous environments. These may take the form of the reported subglacial lake at the Martian south pole³, or the deep groundwater beneath the Martian cryosphere². These cold environments have been hypothesised to contain high concentrations of perchlorate salts, following their detection at the surface⁶, due to their extremely low eutectic temperatures. Perchlorate salts have been shown to have deleterious effects on microbial life^{7,8} and so must be considered as a factor that will shape the habitability of these environments. In addition to perchlorate salts, sulphates are widely distributed across the Martian surface⁹ and so provide a useful comparison for Mars relevant salt effects on biochemistry. The Martian groundwater would experience pressures of \sim 100 MPa (1 kbar) at the base of the cryosphere at the Martian poles if it reached a depth of 10 km². Thus, to be able to assess the habitability of subsurface environments, we must investigate the combination of strong ionic effects and high pressures. Though there is quite a lot known about the effects cellular organic osmolytes, such as trimethylamine-*N*-oxide, impose on organisms thriving in the deep sea under high-pressure stress up to the 1000 bar level^{10–12}, the combined effects of high salt, low temperature, and high pressure on biochemical processes is still terra incognita.

Previous studies have demonstrated the deleterious effects of destabilising ions such as perchlorates on the activity of α -chymotrypsin (α -CT) and other enzymes^{7,13}. Conversely, stabilising salts, such as sodium sulphate¹⁴, have been shown to increase the activity and structural stability of α -CT¹⁵. Our knowledge of how these molecules affect enzyme activity is largely restricted to ambient temperatures and pressures. Therefore, a greater understanding of how these effects change with pressure is yet to be achieved.

The effect of pressure on enzyme kinetics is largely dictated by Le Châtelier's principle. If an enzymatic reaction exhibits a negative change in volume ($\Delta V < 0$), or negative activation volume ($\Delta V^\ddagger < 0$), the overall reaction yield and rate will increase in that direction. A negative volume change is achieved when the volume occupied by the enzyme-substrate complex (ES) is lower than that of the enzyme (E) and substrate (S) in solution. The same holds true for negative activation volumes, which occur when the activated transition state (TS) occupies a lower volume than the ES complex. Previous studies have shown that α -CT exhibits a negative activation volume and, as such, its activity increases with pressure^{16–18}.

In this work, the effects that Mars relevant salts (MgSO_4 and $\text{Mg}(\text{ClO}_4)_2$) and high hydrostatic pressures exert on the activity and structural stability of α -CT, an archetype of a digestive enzyme, are explored. Assayed concentrations of MgSO_4 and $\text{Mg}(\text{ClO}_4)_2$ of 0.25 and 0.5 M allow for a comparison of the effects of both salts on our system as concentrations of $\text{Mg}(\text{ClO}_4)_2 > 1$ M induce unfolding of α -CT at room temperature. This work advances our understanding of how the interactions of high concentrations of these ions and high pressure influence the biochemistry and habitability of terrestrial and extraterrestrial environments.

Results

α -chymotrypsin activity in Mars salts. The effects of pressure and high concentrations of Mars relevant salts on enzymes has not been previously investigated. The Michaelis–Menten plots in Fig. 1 show the activity of α -CT in the absence and presence of MgSO_4 and $\text{Mg}(\text{ClO}_4)_2$. The activity of α -CT increases with pressure, as has been previously described^{16–18}. Figure 2a, b show that the Michaelis constant, K_M , decreases slightly with increasing pressure, i.e., the affinity of the substrate increases slightly upon compression. The turnover number, k_{cat} , increases about 2–3 fold and the catalytic efficiency, $k_{\text{cat}}/K_M = k_{\text{eff}}$, rises by a factor of 5 in all solutions upon compression from 1 to 2000 bar. Table SI1 lists the kinetic parameters of k_{cat} , K_M and k_{cat}/K_M for α -CT in buffer in the absence and presence of MgSO_4 and $\text{Mg}(\text{ClO}_4)_2$. The data show that the k_{cat} of α -CT is lower at each pressure step at both $\text{Mg}(\text{ClO}_4)_2$ concentrations than when in buffer alone. Despite the lower k_{cat} values, the reduced K_M values result in a greater catalytic efficiency (k_{cat}/K_M) for α -CT at 2000 bar in 0.25 M $\text{Mg}(\text{ClO}_4)_2$ compared to buffer, whereas the catalytic efficiency is reduced at 2000 bar in 0.5 M $\text{Mg}(\text{ClO}_4)_2$. The activity of α -CT is also increased in the presence of MgSO_4 at both concentrations with greater k_{cat} values above 1 bar, lower K_M values, and greater catalytic efficiency.

The change in the kinetic parameters, in both real numbers and as percentages, are presented in Fig. 2a–f. The greatest proportional change in k_{cat} from 1 to 2000 bar is in the presence of 0.25 M $\text{Mg}(\text{ClO}_4)_2$ (+144%), the greatest proportional change in K_M is in buffer (−76.5%) and the greatest proportional change in k_{cat}/K_M observed is in 0.25 M MgSO_4 (+466%).

Figure 2g and Table SI2 show the data for the activation volume, which were determined using Eq. (2) (see below). All ΔV^\ddagger values exhibit a negative value (order of magnitude, $-8 \dots -11 \text{ cm}^3 \text{ mol}^{-1}$), which is similar to that described in the literature^{19,20}. Furthermore, the ΔV^\ddagger slightly increases with increasing substrate concentration (Table SI3), reaching plateau values for substrate concentrations of about 2 mM, i.e., for concentrations where the enzyme is saturated with substrate. The activation volume for large substrate concentrations, where $v_0 \propto k_{\text{cat}}$, describes the difference in the volumes of the TS and the ES complex, i.e., $\Delta V^\ddagger = V^\ddagger - V_{\text{ES}}$, whereas measuring the activation volume at low substrate concentrations, where $v_0 \propto k_{\text{cat}}/K_M$, includes the volume change due to substrate binding, i.e., $\Delta V^\ddagger = V^\ddagger - V_{\text{E}+\text{S}}$ ^{21,22}. The latter contribution seems to depend slightly on the particular solution conditions and amounts to about -4 to $-6 \text{ cm}^3 \text{ mol}^{-1}$, i.e., the ES substrate complex is slightly more compact relative to the partial volumes of enzyme and substrate,

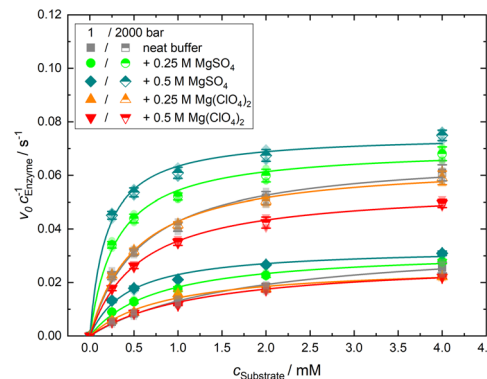


Fig. 1 α -Chymotrypsin activity curves. Michaelis–Menten plots of the enzymatic activity of α -CT at $T = 20$ °C in different buffer solutions at two selected pressures, 1 bar and 2 kbar. Error bars represent standard deviation.

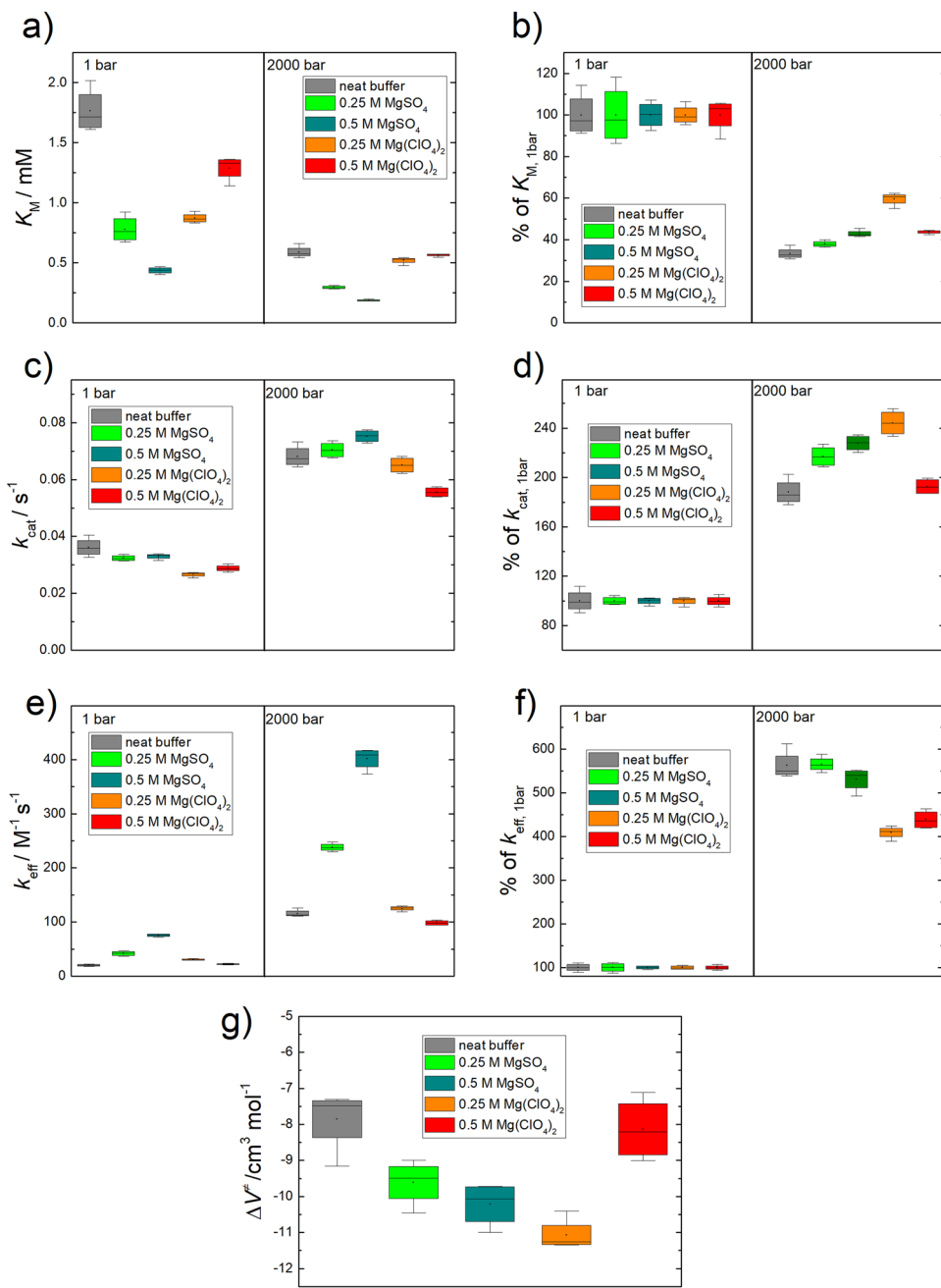


Fig. 2 Kinetic and volumetric parameters of α -chymotrypsin activity. a, c, e Pressure dependence of the kinetic parameters (K_M , k_{cat} and $k_{\text{eff}} = k_{\text{cat}}/K_M$) of the α -CT-catalysed hydrolysis reaction of SPpNA in different salt conditions. **b, d, f** Each salt condition was normalised to its own kinetic parameter at 1 bar (starting point: 100%). Activation volume at high substrate concentrations, reflecting **(g)** the volume change responsible for k_{cat} . Error bars represent standard deviation.

probably due to partial desolvation upon substrate binding. $\Delta V'$ values for all salt conditions reveal no significant differences compared to the neat buffer. Altogether, the TS is more compact than the ES complex, which might be due to a decrease of void volume and/or hydration of charges (electrostriction effect) in the TS.

The difference in the effect of both salts is largely attributable to the extent to which they preferentially interact with the peptide backbone (perchlorate) or are excluded from the peptide surface (sulphate)²³. It is also worth noting that while this can be examined as an anion or cation effect, it is worth considering the whole salt due to the varied extent with which the ions pair with each other in water²⁴.

Pressure–temperature stability of α -chymotrypsin. To follow the temperature- and pressure-dependent unfolding process of α -CT in detail, the secondary structural changes in the presence of perchlorate compared to neat buffer (+10 mM CaCl_2) were measured using Fourier-transform infrared (FTIR) spectroscopy, covering a temperature range from 20 to 70 °C and a pressure range from 1 bar to 10 kbar (1 GPa). Figure 3 displays the normalised temperature-dependent FTIR spectra of α -CT (Fig. 3a, c, e) as well as the corresponding changes in secondary structural elements (Fig. 3b, d, f) for different concentrations of perchlorate. At ambient pressure and 20 °C, the amide I' band of α -CT in neat buffer shows a broad band at 1638 cm^{-1} , with aggregation bands appearing at 1617 cm^{-1} and 1684 cm^{-1} at high temperatures. The

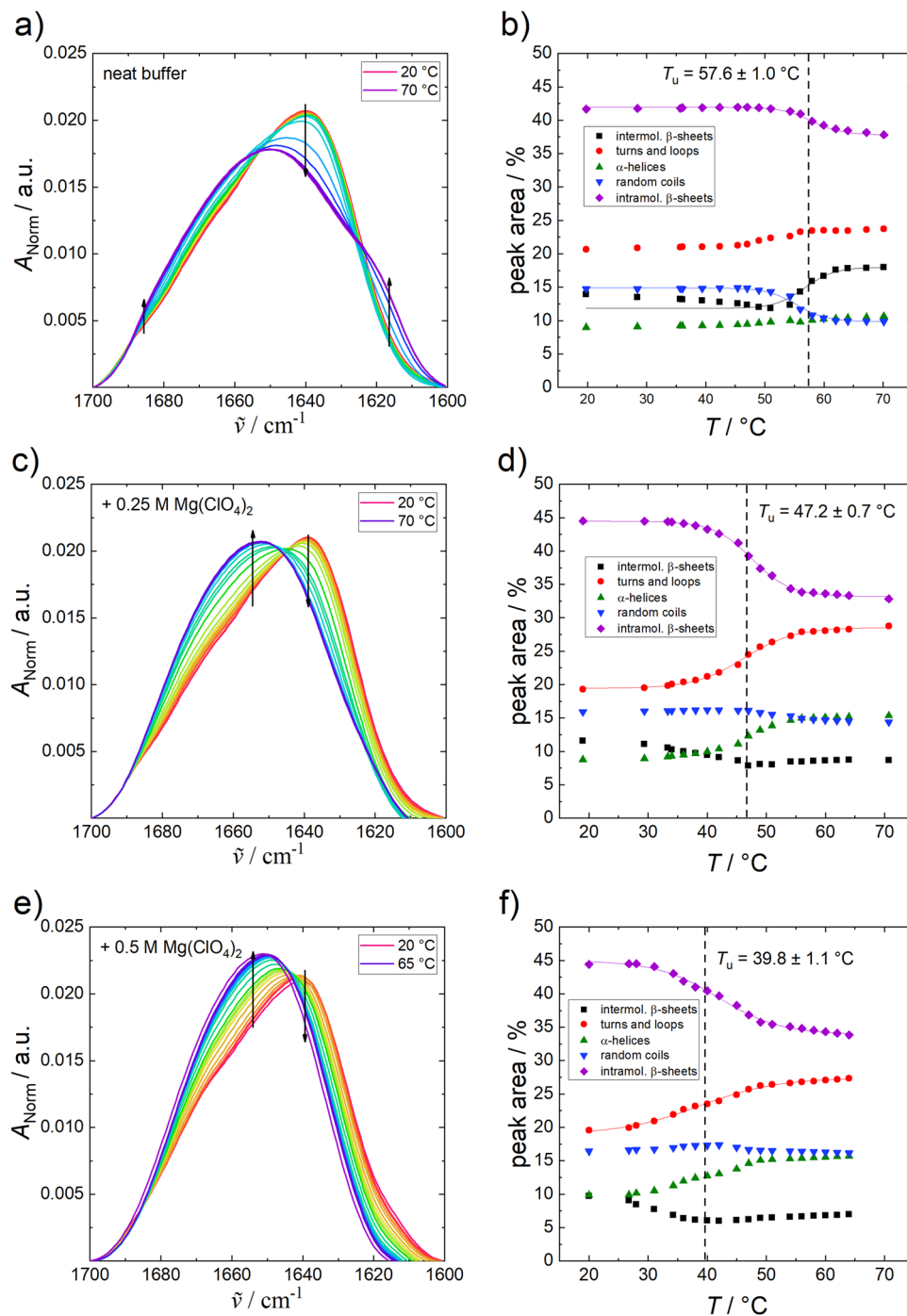


Fig. 3 Changes to α -chymotrypsin FTIR spectra with temperature. Normalised temperature-dependent FTIR spectra of α -CT (50 mg mL⁻¹) in neat buffer (+10 mM CaCl₂) (a), 0.25 M (c) and 0.5 M Mg(ClO₄)₂ (e) at ambient pressure and the corresponding secondary structural changes (b, d, f) obtained from the curve fitting procedure. Arrows indicate increasing temperature and the lines represent the Boltzmann fits to the experimental data using Eq. (3).

secondary structure components obtained, which are derived from the curve fitting procedure (Fig. 3b), are in accord with earlier results reported by Meersman et al.²⁵ At ambient pressure and 25 °C, α -CT shows high contents of intramolecular β -sheets (~43%) and turns and loops (~21%) and lower amounts of α -helices (~9%). These results are in rather good agreement with crystallographic data²⁶. The minor differences between the X-ray diffraction and FTIR results (see Table SI 4) may be due to different absorption coefficients of the various secondary structure elements, which is not significant as only relative changes are

essentially discussed here. Upon temperature-induced unfolding/denaturation, the intramolecular β -sheet content decreases (~5%) and aggregation of the protein via formation of intermolecular β -sheets (~+5%) takes place in neat buffer (Fig. 3b).

Remarkably, in the presence of Mg(ClO₄)₂, no aggregation via formation of intermolecular β -sheets occurs upon unfolding at high temperatures. The intramolecular β -sheet content decreases and the α -helices & turns/loops content increases concomitantly. With increasing perchlorate concentration, the unfolding temperature, T_u , of α -CT decreases from 57.6 °C to 39.8 °C, i.e., the

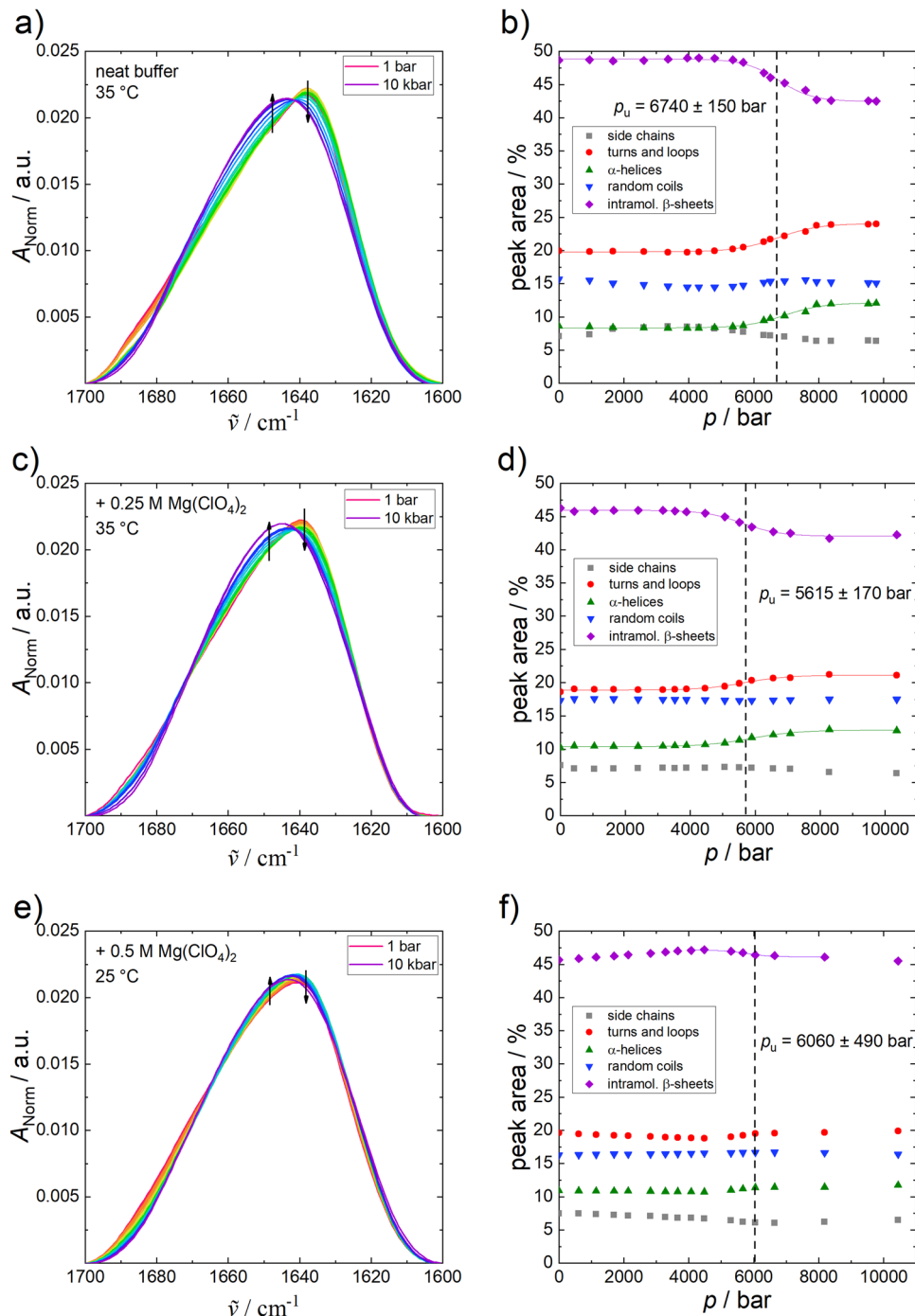


Fig. 4 Changes to α -chymotrypsin FTIR spectra with pressure. Normalised pressure-dependent FTIR spectra of α -CT (50 mg mL^{-1}) in (a) neat buffer ($+10 \text{ mM CaCl}_2$) (a), (c) $0.25 \text{ M Mg}(\text{ClO}_4)_2$ and (e) at 35°C , $0.5 \text{ M Mg}(\text{ClO}_4)_2$ at 25°C , and the corresponding secondary structural changes (b, d, f) obtained from the curve fitting procedure. Arrows indicate increasing pressure and lines show the Boltzmann fits to the experimental data using Eq. (4).

salt leads to a marked destabilization of the temperature stability of the protein. Further, the width of the unfolding transition region increases upon addition of perchlorate, pointing to a decreasing cooperativity of the transition.

Figure 4 depicts the normalised pressure-dependent FTIR spectra of α -CT (Fig. 4a, c, e) and the corresponding secondary structural changes (Fig. 4b, d, f) at different concentrations of perchlorate at 35°C up to 10 kbar . With increasing pressure in neat buffer solution, the amide I' band of α -CT shifts to higher wavenumbers and partial unfolding is observed at around 6700

bar. Regarding the relative changes of secondary structure elements, the α -helix & turns/loops content increases ($\sim +4\%$), while the percentage of intramolecular β -sheets decreases ($\sim -4\%$) concomitantly upon compression. In the presence of $0.25 \text{ M Mg}(\text{ClO}_4)_2$, the secondary structural changes are similar, and α -CT partially unfolds at a lower pressure (5600 bar , 35°C) compared to the buffer condition. In summary, the enzyme is very pressure stable, even in the presence of 0.25 M of perchlorate. The temperature- and pressure-induced (partial) denaturation is irreversible for all conditions measured.

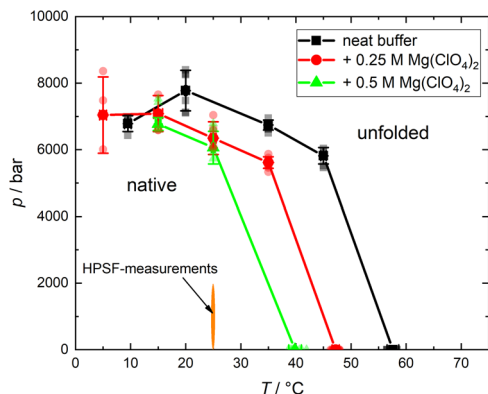


Fig. 5 *p, T*-stability phase diagram of α -chymotrypsin. p, T -stability phase diagram of α -chymotrypsin (50 mg mL^{-1} , 10 mM CaCl_2). The lines indicate the transition curve, where $\Delta G_u = 0$, i.e., show the transition from the native to the (partially) unfolded state. The kinetic high-pressure stopped-flow (HPSF) measurements were performed in a region where the protein is well within the natively folded state. Error bars represent standard deviation.

Contrary to the conformational entropy gain of the peptide chain, which is the main driving force for the temperature-induced unfolding of proteins, volume changes and compressibility play a decisive role for the pressure-induced unfolding process, where the system tends to occupy an overall smaller volume state at high pressure^{27,28}. To gain a quantitative measure, the volume change of (partial) unfolding, ΔV_u , was determined using Eq. (4). For the partial unfolding of α -CT at 35°C in the absence of $\text{Mg}(\text{ClO}_4)_2$, a value of $\Delta V_u = -41 \pm 7 \text{ cm}^3 \text{ mol}^{-1}$ was obtained, which is consistent with the volume change of the precursor (chymotrypsinogen) of α -CT²⁹ and a typical value observed for unfolding of monomeric proteins^{28,30–32}. At lower temperatures (25°C) or higher perchlorate concentrations (0.5 M), smaller changes in the secondary structure elements are observed upon pressure-induced unfolding, which is reflected in smaller ΔV_u values.

The p, T -phase diagram of α -CT in the absence and presence of $\text{Mg}(\text{ClO}_4)_2$, resulting from these temperature- and pressure-dependent FTIR measurements, is depicted in Fig. 5. At low temperatures and pressures, the native state of the protein is favoured. Crossing the transition line to the unfolded state, the native conformation loses its stability and the protein partially unfolds, losing its enzymatic activity. As is clearly seen from the figure, increasing the perchlorate concentration reduces the pressure and temperature stability of the protein, shifting the boundary to lower values of temperature and pressure. However, the enzyme is stable in the whole p, T -range covered in the HPSF studies, and also in the presence of the two salts.

Literature data on the phase diagram of the α -CT only exists for solution conditions different from ours. The protein unfolds in the absence of Ca^{2+} at 4.9 kbar for $T = 21^\circ\text{C}$ and at 41°C for ambient pressure conditions³³. As expected, Ca^{2+} ions have a positive effect on the temperature and pressure stability of the protein, probably by electrostatic screening of negatively charged surface patterns of the protein. A stabilising effect of Ca^{2+} ions on α -CT has been observed in other unfolding studies of proteins as well^{34,35}. A marked destabilising effect of perchlorate, being a typical low-charge-density anion at the far end of the Hofmeister series of anions, at high concentrations, has been observed in lysozyme at $\text{pH } 7$ as well and is expected to be due to weak binding of the ClO_4^- anions to the protein^{36,37}. This reduces the

Gibbs energy associated with hydrating of the newly exposed interior of the protein upon unfolding, thereby destabilising the native protein's fold. As has been shown recently by Dougan et al.³⁸, the water structure also changes markedly at the high perchlorate concentrations mimicking conditions in Martian soil. They found that the tetrahedral structure of water is heavily perturbed, the effect being equivalent to pressurising pure water to pressures of the order of 20 kbar and more. Interestingly, the Mg^{2+} and ClO_4^- ions appear charge-ordered and bridged by water molecules under these conditions, thereby preventing ice formation at low temperatures.

Discussion

Little is known about the effects of high ion concentrations on cellular life or the combined effects of ions with high pressure. Yet these combinations can shape the habitability of deep subsurface environments on Earth and potentially elsewhere. Currently, one scientific question of great interest is the habitability of the Martian subsurface. Although the question of whether there is life on Mars remains speculative, we can ask questions about how physical and chemical conditions expected on Mars might theoretically influence its habitability. We can then use terrestrial organisms and biomolecules to explore the boundary space of habitability for known life under said Martian conditions. In this study, we used a well characterised enzyme to investigate the combined effects of perchlorate ions and high pressures as a general proxy for biomolecular stability under these extremes.

From the Michaelis-Menten plots it is demonstrable that increasing the hydrostatic pressure also increases the enzyme activity of α -CT, even in the presence of high concentrations of the chaotropic salt $\text{Mg}(\text{ClO}_4)_2$. As α -CT has a negative activation volume ($\Delta V^\ddagger < 0$), the increasing activity with pressure is largely attributed to Le Châtelier's principle as previously described^{16–18}.

From the kinetic parameters it is also shown that $\text{Mg}(\text{ClO}_4)_2$ reduces the activity of α -CT at both concentrations, 0.25 and 0.5 M , and across all pressure conditions tested. This agrees with previous ambient pressure studies showing the same effect of perchlorate salts on α -CT and other enzymes^{7,13}. Furthermore, the observation that MgSO_4 increases the activity of α -CT agrees with previous studies which show that the sulphate ion can stabilise proteins¹⁴ and increase the activity of α -CT¹⁵. This sulphate-induced effect is also shown to be substrate dependent as it was absent in a previous kinetic study using *N*-benzoyl-*L*-tyrosine ethyl ester as the substrate.

Different proportional increases in k_{cat} were observed in response to increasing hydrostatic pressure for the different salt conditions. From previous work at atmospheric pressure it has been shown that perchlorate salts reduce the structural stability of α -CT. It may therefore be the case that high pressures can partially undo this negative structural effect, manifesting itself as the greater proportional increase in k_{cat} . In essence, lesser salt-induced structural disruption at higher pressures may confer greater than expected activity increases than due to Le Châtelier's principle alone. This suggests the existence of an advantageous salt-pressure-activity interplay.

The shift of the α -CT pressure-temperature stability diagram to lower pressures and temperatures with increasing $\text{Mg}(\text{ClO}_4)_2$ concentration also suggests that the region of peak stability is concomitantly shifting to the left also. Therefore, in the presence of $\text{Mg}(\text{ClO}_4)_2$, the region of peak α -CT activity and stability may be found at elevated pressures, and lower temperatures.

It is of interest to note that the pressure-temperature phase diagram of life resembles that of proteins, which is due to the

particular temperature dependence of the proteins' specific heat of unfolding³⁹. Life and proteins both exhibit similar, curved pressure-temperature phase diagrams, whereas lipids and nucleic acids generally have linear pressure-temperature phase diagrams^{28,40,41}. If we were to imagine a *z*-axis emerging from Fig. 5 representing the (standard) free energy of unfolding (ΔG_u), we would be able to see the protein stability phase space as a function of free energy also. In this phase diagram, α -CT would exhibit a peak of stability (maximum of ΔG_u) which descends down to the measured unfolding pressures and temperatures where $\Delta G_u = 0$. It would be interesting to know how the perchlorate salts affect the position of the region of peak stability. If it was found that the perchlorate salt moves the region of peak stability to higher than ambient pressures and lower temperatures, is it also moving the region of peak fitness for life? If so, it would suggest that life is more favourable in perchlorate brines if they also experience increased pressures and lower temperatures (a similar salinity-pressure-temperature-growth relationship has been described by Kaye and Baross⁴²). It is then of interest that such environments have either been potentially observed or theorised to be present on Mars^{2,3}. Therefore, whilst concentrated perchlorate brines reduce the habitability of an aqueous environment, high pressures and lower temperatures may counteract the deleterious perchlorate effect, thus increasing habitability. There is already tentative evidence showing that sub 0 °C temperatures confer greater survival of bacteria in perchlorate brines⁴³.

While the effects of low temperatures on our model enzyme in the presence of perchlorate salts remains unknown, we have shown that high pressures can still increase enzyme activity even in the presence of a destabilising salt predicted to be concentrated on Mars. Moreover, high pressures may confer greater structural stability, reducing the destabilising effects of perchlorate salts on proteins. It would be of particular interest to expand our understanding of the perchlorate-pressure-temperature effect on membrane proteins as, in addition to secreted biomolecules, they would be directly exposed to the perchlorate-rich environment. Thus, the effect that concentrated perchlorate salts exert on processes such as molecular transport and signalling may be of particular importance to habitability. Finally, similar to the case of the enzymes of extremely halophilic archaea⁴⁴, changes in amino acid composition under such high $Mg(ClO_4)_2$ concentrations, e.g., by changing the ratio of negatively to positively charged and hydrophobic residues⁴⁴, might help in optimising enzymatic activity under such harsh salt concentrations.

Methods

Materials. Lyophilised α -chymotrypsin from bovine pancreas, Tris (Tris(hydroxymethyl)aminomethane) as well as the salts $MgSO_4$, $Mg(ClO_4)_2$ and $CaCl_2$ were obtained from Sigma-Aldrich, Germany.

Measuring α -chymotrypsin activity. Enzyme activity was measured using a high-pressure stopped-flow system, HPSF-56, from Hi-Tech Scientific^{16,19,45}. The enzyme was prepared as a 20 μM buffered stock solution (0.1 M Tris-HCl, 0.01 M $CaCl_2$, pH 7.8) in the absence or presence of $MgSO_4$ or $Mg(ClO_4)_2$ at either 0.25 or 0.5 M. Enzyme concentration was measured using its absorbance at 280 nm with a molar extinction coefficient of 51000 $M^{-1} cm^{-1}$. Stock solutions of N-Succinyl-Phe-*p*-nitroanilide (SPpNA) were prepared at 8 mM in the same buffer and salt concentrations as enzyme stock solutions. The enzyme concentration was maintained at 10 μM post-mixing for all activity assays with post-mixing substrate concentrations of 0.25, 0.5, 1, 2 and 4 mM. The pressures assayed were 1, 500, 1000, 1500 and 2000 bar. The reaction was monitored for 50 s post-mixing as the change in absorbance at 410 nm due to the formation of the reaction product *p*-nitroaniline, which has a molar extinction coefficient of 8800 $M^{-1} cm^{-1}$. Temperature was controlled and maintained at 20 °C by a thermostat.

The enzyme activity was plotted in Origin 9.3 (OriginLab) and a least-squares fit fitting method was applied according to the Michaelis-Menten equation:

$$v = \frac{v_{max}[S]}{K_M + [S]} \quad (1)$$

The Eyring-equation describes the pressure effect on the rate of the reaction⁴⁶:

$$\left(\frac{\partial \ln(k/k_0)}{\partial p} \right)_T = -\frac{\Delta V^*}{RT} \quad (2)$$

(p = pressure, T = temperature, R = ideal gas constant, ΔV^* = activation volume, k_0 = rate constant at a reference pressure, 1 bar). Within the framework of the Michaelis-Menten formalism, $k = k_{cat}$, when the substrate concentration is large, and $k = k_{cat}/K_M$, when the substrate concentration, $[S]$, is small. The activation volume describes the difference of the volume of the TS and the ground state (ES) of the ES complex or the reactants E and S. Due to different compressibilities of the reactants, the ES complex and the TS, ΔV^* values can be positive or negative, and they may also be dependent on the pressure amplitude.

FTIR: Sample preparation and secondary structure analysis. The enzyme α -chymotrypsin from bovine pancreas was purchased from Sigma-Aldrich as lyophilized powder. For H/D-exchange, the protein was dialysed against D_2O using Amicon Ultra (2 mL) centrifugation units with 10 kDa cut-off and subsequently lyophilized. For the pressure dependent FTIR spectroscopy studies, the measurements were carried out in 100 mM Tris (Tris(hydroxymethyl)aminomethane) buffer with 10 mM $CaCl_2$ in the absence and in the presence of $Mg(ClO_4)_2$. For the temperature-dependent experiments, phosphate buffer was used. The pD-value of both buffers was adjusted to 7.8 (pH + 0.4 = pD) by adding DCl. All chemicals were used without further purification.

FTIR spectra were collected using a Nicolet 6700 (Thermo Fisher Scientific) equipped with a liquid-nitrogen cooled MCT-detector (HgCdTe), operated at -196 °C, in the wavenumber range between 4000 and 650 cm^{-1} . The sample chamber was continuously purged with CO_2 -free and dry air. All measured spectra were averaged over 128 scans in a row at a spectral resolution of 2 cm^{-1} and were processed with Happ-Genzel apodization by using Omnic 7.2 spectral processing software. The equilibration time before each spectrum was recorded at each temperature was 15 min, for the pressure dependent studies 5 min. The temperature IR cell consists of two CaF_2 windows separated by a mylar spacer of 50 μm thickness. The setup of the pressure system consists of a membrane-driven diamond anvil cell (VivoDac Diacell[®]) with type IIa diamonds, which is connected to an automated pneumatic pressure control (Diacell[®] iGM Controller, Almax easyLab). To measure the pressure inside the cell, by adding $BaSO_4$, the pressure-sensitive stretching vibration of SO_4^{2-} (~983.5 cm^{-1} ± 1 bar, 25 °C) was used as an internal pressure calibrator⁴⁷. For each measurement, a protein concentration of 5 wt.% was used and the temperature of the cell was regulated with an external, circulating water thermostat. Processing and analysis of the spectra was carried out with the Grams AI 8.0 software (Thermo Fisher Scientific). Depending on the sample, spectra of the buffer systems were subtracted from the spectra recorded and smoothed afterwards. Then, the area of the amide I' band (1700–1600 cm^{-1} , which is essentially based on the conformation sensitive C=O stretching vibration of the peptide bonds) was normalised to 1. Due to small variations in molecular geometry and hydrogen bonding patterns, it is possible to analyse the secondary structural composition and conformational changes of proteins⁴⁸. The number of subbands and their positions for fitting were obtained via Fourier self-deconvolution (FSD) and 2nd derivative approaches. Eight subbands, similar to the results described in the literature²⁵ were obtained and mixed Gaussian-Lorentz functions were used to fit the peak areas in the amide I' band region and to determine the relative changes in the population of secondary structure elements (curve fitting)⁴⁹. Assuming a two-state unfolding process of the protein, a Boltzmann function can be fitted to the temperature- and pressure-dependent sigmoidal curve progression of the intensity changes:

$$I = \frac{I_f - I_u}{1 + e^{-\left(\frac{1}{T_u} - \frac{1}{T}\right) \frac{\Delta H_{vH,u}}{R}}} + I_u, \quad (3)$$

$$I = \frac{I_f - I_u}{1 + e^{-\left(p - p_u\right) \frac{\Delta V_u}{RT}}} + I_u, \quad (4)$$

where I_f and I_u are the plateau values of the IR band intensities, I , of the folded and unfolded protein. The unfolding temperature, T_u , and unfolding pressure, p_u , were obtained from the inflection points of the sigmoidal curves. In addition, the thermodynamic parameters $\Delta H_{vH,u}$ and ΔV_u , i.e., the corresponding van't Hoff enthalpy and volume changes, respectively, can be directly obtained from the fits of the temperature- and pressure-dependent FTIR data.

Statistics and reproducibility. The enzyme activity results represent two biological replicates, each made of two technical replicates. The structural FTIR results represent triplicate measurements. No data points were excluded from the respective analyses.

Reporting summary. Further information on research design is available in the Nature Research Reporting Summary linked to this article.

Data availability

The source data for the figures presented in this study have been included as a supplementary file.

Received: 15 May 2020; Accepted: 10 September 2020;

Published online: 02 October 2020

References

- Chaplin, M. Do we underestimate the importance of water in cell biology? *Nat. Rev. Mol. Cell Biol.* **7**, 861–866 (2006).
- Clifford, S. M. et al. Depth of the Martian cryosphere: revised estimates and implications for the existence and detection of subpermafrost groundwater. *J. Geophys. Res.* **115**, E07001 (2010).
- Orosei, R. et al. Radar evidence of subglacial liquid water on Mars. *Science* **361**, 490–493 (2018).
- Merino, N. et al. Living at the extremes: extremophiles and the limits of life in a planetary context. *Front. Microbiol.* **10**, 780 (2019).
- Harrison, J. P., Gheeraert, N., Tsigelnitskiy, D. & Cockell, C. S. The limits for life under multiple extremes. *Trends Microbiol.* **21**, 204–212 (2013).
- Hecht, M. H. et al. Detection of perchlorate and the soluble chemistry of martian soil at the phoenix lander site. *Science* **325**, 64–67 (2009).
- Laye, V. J. & DasSarma, S. An Antarctic Extreme Halophile and Its Polyextremophilic Enzyme: effects of perchlorate salts. *Astrobiology* **18**, 412–418 (2018).
- Stevens, A. H. et al. Growth, Viability, and Death of Planktonic and Biofilm *Sphingomonas desiccabilis* in Simulated Martian Brines. *Astrobiology* **19**, 87–98 (2019).
- Gendrin, A. et al. Sulfates in Martian layered terrains: the OMEGA/Mars express view. *Science* **307**, 1587–1591 (2005).
- Yancey, P. H. & Siebenaller, J. F. Co-evolution of proteins and solutions: protein adaptation versus cytoprotective micromolecules and their roles in marine organisms. *J. Exp. Biol.* **218**, 1880–1896 (2015).
- Daniel, I., Oger, P. & Winter, R. Origins of life and biochemistry under high-pressure conditions. *Chem. Soc. Rev.* **35**, 858–875 (2006).
- Meersman, F. et al. High-pressure biochemistry and biophysics. *Rev. Mineral. Geochem.* **75**, 607–648 (2013).
- Warren, J. C. & Cheatum, S. G. Effect of neutral salts on enzyme activity and structure *. *Biochemistry* **5**, 1702–1707 (1966).
- Cozzolino, S., Oliva, R., Graziano, G. & Del Vecchio, P. Counteraction of denaturant-induced protein unfolding is a general property of stabilizing agents. *Phys. Chem. Chem. Phys.* **20**, 29389–29398 (2018).
- Dušeková, E., Garajová, K., Yavaşer, R., Varhač, R. & Sedláček, E. Hofmeister effect on catalytic properties of chymotrypsin is substrate-dependent. *Biophys. Chem.* **243**, 8–16 (2018).
- Luong, T. Q. & Winter, R. Combined pressure and cosolvent effects on enzyme activity - A high-pressure stopped-flow kinetic study on α -chymotrypsin. *Phys. Chem. Chem. Phys.* **17**, 23273–23278 (2015).
- Luong, T. Q., Kapoor, S. & Winter, R. Pressure-A gateway to fundamental insights into protein solvation, dynamics, and function. *ChemPhysChem* **16**, 3555–3571 (2015).
- Knierbein, M. et al. Combined co-solvent and pressure effect on kinetics of a peptide hydrolysis: an activity-based approach. *Phys. Chem. Chem. Phys.* **21**, 22224–22229 (2019).
- Mozhaev, V. V., Lange, R., Kudryashova, E. V. & Balny, C. Application of high hydrostatic pressure for increasing activity and stability of enzymes. *Biotechnol. Bioeng.* **52**, 320–331 (1996).
- Jaworek, M. W., Schuabb, V. & Winter, R. The Effects of Glycine, TMAO and Osmolyte Mixtures on the Pressure Dependent Enzymatic Activity of α -Chymotrypsin. *Phys. Chem. Chem. Phys.* **20**, 1347–1354 (2017).
- Schuabb, V., Winter, R. & Czeslik, C. Improved activity of α -chymotrypsin on silica particles - a high-pressure stopped-flow study. *Biophys. Chem.* **218**, 1–6 (2016).
- Butz, P., Greulich, K. O. & Ludwig, H. Volume changes during enzyme reactions: indications of enzyme pulsation during fumarate catalysis. *Biochemistry* **27**, 1556–1563 (1988).
- Pegram, L. M. & Record, M. T. Jr Quantifying accumulation or exclusion of H (+), HO (-), and Hofmeister salt ions near interfaces. *Chem. Phys. Lett.* **467**, 1–8 (2008).
- Held, C. & Sadowski, G. Modeling aqueous electrolyte solutions. Part 2. Weak electrolytes. *Fluid Phase Equilib.* **279**, 141–148 (2009).
- Meersman, F., Dirix, C., Shipovskov, S., Klyachko, N. L. & Heremans, K. Pressure-induced protein unfolding in the ternary system AOT-octane-water is different from that in bulk water. *Langmuir* **21**, 3599–3604 (2005).
- Levitt, M. & Greer, J. Automatic identification of secondary structure in globular proteins. *J. Mol. Biol.* **114**, 181–293 (1977).
- Akasaka, K. & Matsuki, H. *High Pressure Bioscience Biomedical and Life Sciences* (Springer Science & Business Media, Dordrecht, 2015). <https://doi.org/10.1007/978-94-017-9918-8>.
- Winter, R. Interrogating the structural dynamics and energetics of biomolecular systems with pressure modulation. *Annu. Rev. Biophys. Biomol. Struct.* **48**, 441–463 (2019).
- Hawley, S. A. Reversible pressure-temperature denaturation of chymotrypsinogen. *Biochemistry* **10**, 2436–2442 (1971).
- Roche, J. et al. Cavities determine the pressure unfolding of proteins. *PNAS* **109**, 6945–6950 (2012).
- Silva, J. L. et al. High-Pressure Chemical Biology and Biotechnology. *Chem. Rev.* **114**, 7239–7267 (2014).
- Gao, M. et al. Crowders and Cosolvents—Major Contributors to the Cellular Milieu and Efficient Means to Counteract Environmental Stresses. *ChemPhysChem* **18**, 2951–2972 (2017).
- Sun, Z. & Winter, R. Temperature- and Pressure-induced Unfolding of α -Chymotrypsin. *Advances in High Pressure Bioscience and Biotechnology II* (ed. Winter, R.) (Springer, Berlin, Heidelberg, 2002).
- Kar, K., Alex, B. & Kishore, N. Thermodynamics of the interactions of calcium chloride with α -chymotrypsin. *J. Chem. Thermodyn.* **34**, 319–336 (2002).
- Wu, F. C. & Laskowski, M. The effect of calcium on chymotrypsins α and B. *Biochim. Biophys. Acta* **19**, 110–115 (1956).
- Bye, J. W. & Falconer, R. J. Thermal stability of lysozyme as a function of ion concentration: a reappraisal of the relationship between the Hofmeister series and protein stability. *Protein Sci.* **22**, 1563–1570 (2013).
- Lee, E., Choi, J. H. & Cho, M. The effect of Hofmeister anions on water structure at protein surfaces. *Phys. Chem. Chem. Phys.* **19**, 20008–20015 (2017).
- Lenton, S., Rhys, N. H., Towey, J. J., Soper, A. K. & Dougan, L. Highly compressed water structure observed in a perchlorate aqueous solution. *Nat. Commun.* **8**, 1–5 (2017).
- Smeller, L. Pressure-temperature phase diagrams of biomolecules. *Biochim. Biophys. Acta - Protein Struct. Mol. Enzymol.* **1595**, 11–29 (2002).
- Hawley, S. A. & Macleod, R. M. Pressure-temperature stability of DNA in neutral salt solutions. *Biopolymers* **13**, 1417–1426 (1974).
- Winter, R., Erbes, J., Czeslik, C. & Gabke, A. Effect of pressure on the stability, phase behaviour and transformation kinetics between structures of lyotropic lipid mesophases and model membrane systems. *J. Phys. Condens. Matter* **10**, 11499–11518 (1998).
- Kaye, J. Z. & Baross, J. A. Synchronous effects of temperature, hydrostatic pressure, and salinity on growth, phospholipid profiles, and protein patterns of four *Halomonas* species isolated from deep-sea hydrothermal-vent and sea surface environments. *Appl. Environ. Microbiol.* **70**, 6220–6229 (2004).
- Heinz, J., Schirmack, J., Airo, A., Kounaves, S. P. & Schulze-Makuch, D. Enhanced microbial survivability in subzero brines. *Astrobiology* **18**, 1171–1180 (2018).
- Hochachka, P. W. & Somero, G. N. *Biochemical adaptation: mechanism and process in physiological evolution* (Oxford University Press, 2002).
- Luong, T. Q. et al. Hydrostatic Pressure Increases the Catalytic Activity of Amyloid Fibril Enzymes. *Angew. Chem. - Int. Ed.* **55**, 12412–12416 (2016).
- Eisenmenger, M. J. & Reyes-De-Corcuera, J. I. High pressure enhancement of enzymes: a review. *Enzym. Microb. Technol.* **45**, 331–347 (2009).
- Wong, P. & Moffat, D. A new internal pressure calibrator for high-pressure infrared spectroscopy of aqueous systems. *Appl. Spectrosc.* **43**, 1279–1281 (1989).
- Byler, D. M. & Susi, H. Examination of the secondary structure of proteins by deconvolved FTIR spectra. *Biopolymers* **25**, 469–487 (1986).
- Panick, G. & Winter, R. Pressure-induced unfolding/refolding of ribonuclease A: static and kinetic fourier transform infrared spectroscopy study. *Biochemistry* **39**, 1862–1869 (2000).

Acknowledgements

S.G. and C.S.C. would like to thank the EPSRC for their support. C.S.C. was supported by Science and Technologies Facilities Council grant number: ST/R000875/1. R.W. acknowledges funding from the Deutsche Forschungsgemeinschaft (DFG, German Research Foundation) under Germany's Excellence Strategy – EXC-2033 – Projektnummer 390677874.

Author contributions

S.G. and M.W.J. conducted the experiments. R.W. and C.S.C. supervised the work. All authors contributed to data analysis and the writing of the paper.

Competing interests

The authors declare no competing interests.

Additional information

Supplementary information is available for this paper at <https://doi.org/10.1038/s42003-020-01279-4>.

Correspondence and requests for materials should be addressed to S.G.

Reprints and permission information is available at <http://www.nature.com/reprints>

Publisher's note Springer Nature remains neutral with regard to jurisdictional claims in published maps and institutional affiliations.



Open Access This article is licensed under a Creative Commons Attribution 4.0 International License, which permits use, sharing, adaptation, distribution and reproduction in any medium or format, as long as you give appropriate credit to the original author(s) and the source, provide a link to the Creative Commons license, and indicate if changes were made. The images or other third party material in this article are included in the article's Creative Commons license, unless indicated otherwise in a credit line to the material. If material is not included in the article's Creative Commons license and your intended use is not permitted by statutory regulation or exceeds the permitted use, you will need to obtain permission directly from the copyright holder. To view a copy of this license, visit <http://creativecommons.org/licenses/by/4.0/>.

© The Author(s) 2020